

UNH SEA GRANT PROGRAMS

3 copy

UNH-RAYTHEON SEA GRANT PROJECT

TECHNICAL REPORT

Description of Viscoelastic Properties
of Ocean Sediments via Signal Processing

H. Tugal and M. Yildiz
Mechanics Research Laboratory

A Report of a
Cooperative University-Industry Research Project
between

University of New Hampshire
Durham, New Hampshire

Raytheon Company
Portsmouth, Rhode Island



**UNIVERSITY of NEW HAMPSHIRE
DURHAM, NEW HAMPSHIRE. 03824**

Report No. UNH-SG-147

August 1974

A TECHNICAL REPORT TO
THE NATIONAL SEA GRANT PROGRAM
OF
THE NATIONAL OCEANIC AND ATMOSPHERIC ADMINISTRATION
U. S. DEPARTMENT OF COMMERCE

DESCRIPTION OF VISCOELASTIC PROPERTIES
OF OCEAN SEDIMENTS VIA SIGNAL PROCESSING

by
H. Tugal and M. Yildiz
Mechanics Research Laboratory

This work is a result of research sponsored by NOAA Office of Sea Grant,
Department of Commerce, under Grant No. D of C 04-3-158-69. The U. S.
Government is authorized to produce and distribute reprints for governmental
purposes, notwithstanding any copyright notation that may appear hereon.

Approved:



Musa Yildiz - Technical Director

COOPERATING INSTITUTIONS

University of New Hampshire
Durham, New Hampshire 03824

Submarine Signal Division
Raytheon Company
Portsmouth, Rhode Island 02871

ABSTRACT

The recovery of the essential engineering data necessary for the efficient utilization of the sea floor is tedious and expensive. For this reason we shall employ remote acoustic sensing techniques to estimate the soil parameters.

It is known that the soil parameters, known as the Lamé' parameters (which consist of $(\lambda' + 2\mu')$ real part, and $(\lambda'' + 2\mu'')$ imaginary part of compressional wave parameters, and μ' real part, and μ'' imaginary part shear wave parameters), together with density of the soil " ρ " and the spatial wave number " k " of the waves, completely describe viscoelastic properties of the soil. Hence, it is necessary to make the measurements in such a way that we are able to describe the following parameters λ' , λ'' , μ' , μ'' , ρ , and k .

In this investigation it is shown in a qualitative way that we can relate the directly measurable quantities (such as γ , ζ , Q , ω_c , and $\omega_c(1-\zeta^2)^{\frac{1}{2}}$ as illustrated in Figure (2), (3), (5), and (6)) which are obtained through the data acquisition system (see Figure (1)) to the soil parameters μ' , μ'' , λ' , λ'' , and ρ by developing the field theoretical model which prescribes the viscoelastic soil parameters of the marine sediments (illustrated in Figures (7), (8), and (9)).

INTRODUCTION

Early in this investigation, it was recognized that the widely used ray theory approach to the acoustic-soil mechanical interactions associated with the remote sensing of sea floor parameters would not yield, in all likelihood, increased insights into the basic processes. While the theory has provided substantial understanding in some acoustic fields of study, a theory which is more sensitive to sub-bottom parameters is necessary. A field theoretical approach was pursued early in the project because the all-important physical phenomenology can be included in the analysis. The field theoretical approach is often discarded because of mathematical difficulties. However, when we seek sensitive interrelationships of acoustic and physical parameters in a multi-layered environment, we can not oversimplify the analysis. The emphasis during the first two years has been to overcome the mathematical complexities with simple models, which are increased step by step in complexity until they adequately represent the physical world.

The models, based on the physical configuration shown in Figure (1), have been developed for the full range of equivalent angles of incidence from normal incidence to highly oblique angles. The results obtained are for water depths of 50 to 600 feet (see Figure (3)) and for frequencies (see Figure (3)) of 3 to 20 KHz. The results are for the acoustic response created by a steady state point source in a semi-infinite liquid overlaying of viscoelastic halfspace, with n-layers of differing properties.

In the field theoretical approach, two important measureable parameters are emerged: 1) compressional wave velocity, and 2) sea floor reflection coefficient.

The prototype system (which will be discussed in the subsequent section) provides precise measurement of the compressional wave velocity. It is important to note that the velocity data is collected while conducting conventional sub-bottom profiling with the vessel traveling at speeds up to six knots. The received data involving layer velocity is to be processed using some mathematical technique (layer velocity is determined, for example, employing $T^2 - X^2$ approach of Dobrin and Dix) which is not managable for direct reading purposes.

The reflection coefficient is defined as the ratio of the reflected to the incident signals:

$$R = \frac{\rho_2 a_{L2} - \rho_1 a_{L1}}{\rho_2 a_{L2} + \rho_1 a_{L1}}$$

where

($\rho_{1,2}$ denotes bulk densities and $a_{L1,2}$ compressional wave velocities)

with the magnitude of R a direct function of the change in acoustic impedance (ρa_L) across the reflecting interface (Breslau, 1965, 1967).

*The primary objective of his investigation was to measure the acoustic reflectivity of the sea floor by using normal incidence and also to study its geological significance. A secondary objective was to develop a practical technique that could be used for routine acoustical surveying of sea floor sediments from a vessel under way.

Field theoretical consideration of reflection coefficient is given in reference (2), (5), and (6).

By employing a field theoretical approach, an important variation of the normal incidence reflection coefficient, the simultaneous determination of the changes in reflection intensity as a function of incident angle is also relatable to the various sediment types as detailed by Yildiz, and later by Magnuson, and Magnuson, Stewart, and Newman. Even though in this method all the important physical phenomenology is included in the analysis, there is not a direct correlation between the field theoretical model and the experimental data. Therefore, it was necessary to recast our field approach in such a way that we could correlate the experimental data directly with our field theoretical model. It is further noted (see Figures (2), (3), and (4)) in order to interpret experimental data directly and properly, we have to have an analytical model which relates the attenuation constant γ , the damping factor ζ , the quality factor Q , undamped and damped frequency of compressional wave system (i.e. ω_c , and $\omega_c \sqrt{1 - \zeta^2}$) to the sediment parameters μ' , μ'' , λ' , λ'' , ρ , k which completely describes remotely sub-bottom ocean marine sediments.

The purpose of this investigation is, therefore, to show that we are now able to relate directly the measurable quantities (such as γ , ζ , Q , ω_c , and $\omega_c (1 - \zeta^2)^{\frac{1}{2}}$) obtained through the data acquisition system (see Figure (1)) to the soil parameters μ' , μ'' , λ' , λ'' , and ρ by developing the field theoretical model which prescribes the viscoelastic soil parameters of marine sediments by the following relations:

$$\gamma = \zeta \omega_c = k^2 (\lambda'' + 2\mu'')/2\rho, \quad \zeta = k(\lambda'' + 2\mu'')/2[(\lambda' + 2\mu')\rho]^{1/2}$$

$$Q = [(\lambda' + 2\mu')\rho]^{1/2}/k(\lambda'' + 2\mu''), \quad \omega_c = k(\lambda' + 2\mu'/\rho)^{1/2}$$

$$\omega_c (1 - \zeta^2)^{1/2} = k(\lambda' + 2\mu'/\rho)^{1/2} [1 - (\lambda'' + 2\mu'')^2 k^2 / 4(\lambda' + 2\mu')\rho]^{1/2}$$

It is evident that in this preliminary report, we limited ourselves only to give some qualitative results relevant to sediment classification. In the subsequent papers, we shall discuss the quantitative results in detail.

THE MEASUREMENT SYSTEM

The University of New Hampshire, in conjunction with the Raytheon Company, is engaged in a multi-year study of the application of acoustics to the determination of marine soil's physical and engineering properties. These investigations are conducted under Sea Grant sponsorship. Extensive acoustic and physical data have been acquired as a part of this project. The initial phases of these experimental data acquisition cruises reported in the first annual report, and the details concerning data gathered during the second year are reported elsewhere; but the parts which concern this investigation are summarized here.

An extensive data bank of acoustic signatures for a variety of known sedimentary types has been obtained employing a range of source center frequencies from 3 to 16K HZ. Acoustic sampling were matched with core data to search for acoustical indicators of soil properties and characteristics. For this purpose, a prototype towed-array measurement system has been designed, developed, and tested which provides fundamental data concerning sediments (Figure 1). Incorporated in the array are a series of discrete receiving elements which simultaneously sense the reflected acoustic response of each sedimentary layer over a range of incidence angles. Under normal conditions, this range generally includes angles from zero (normal incidence) up to sixty degrees.

To improve the data measurement precision, the array also incorporates specialized mechanical damping mechanisms and self-contained signal processing; the latter is primarily directed toward S/N improvement. Received signals are further processed by the shipboard portion of the system employing a Raytheon

designed processor which substantially increases the effective dynamic range of the acoustic signals recorded for subsequent computer analysis (see Figure (1)).

Instrumentation described above and computer aided analysis techniques describes an operational remote acoustic sediment classification system. Current output is in the form of digital computer print-out detailing the measured sediment properties as indicated by Figures (2), and (3), and (4) as a time series.

Figures (5) and (6) represent the absolute value of the transfers functions and are obtained from the time series illustrated in Figures (2) and (3), by employing fast-Fourier transform technique.

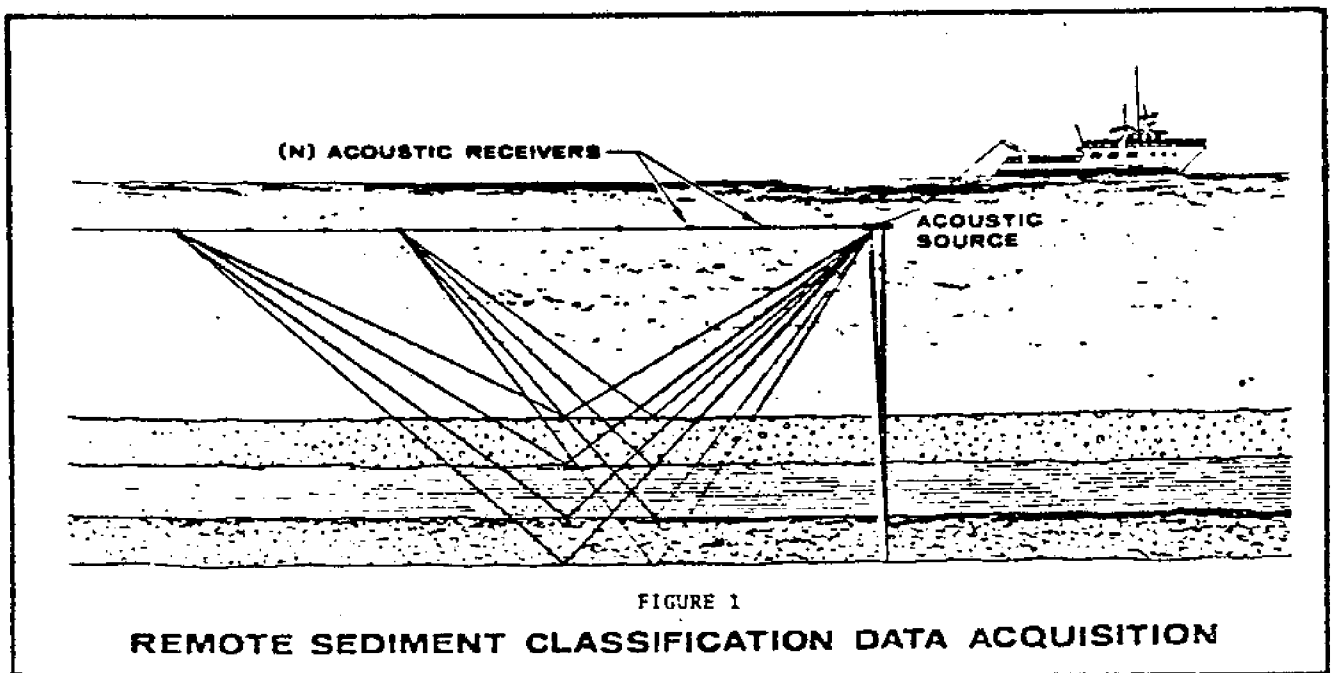
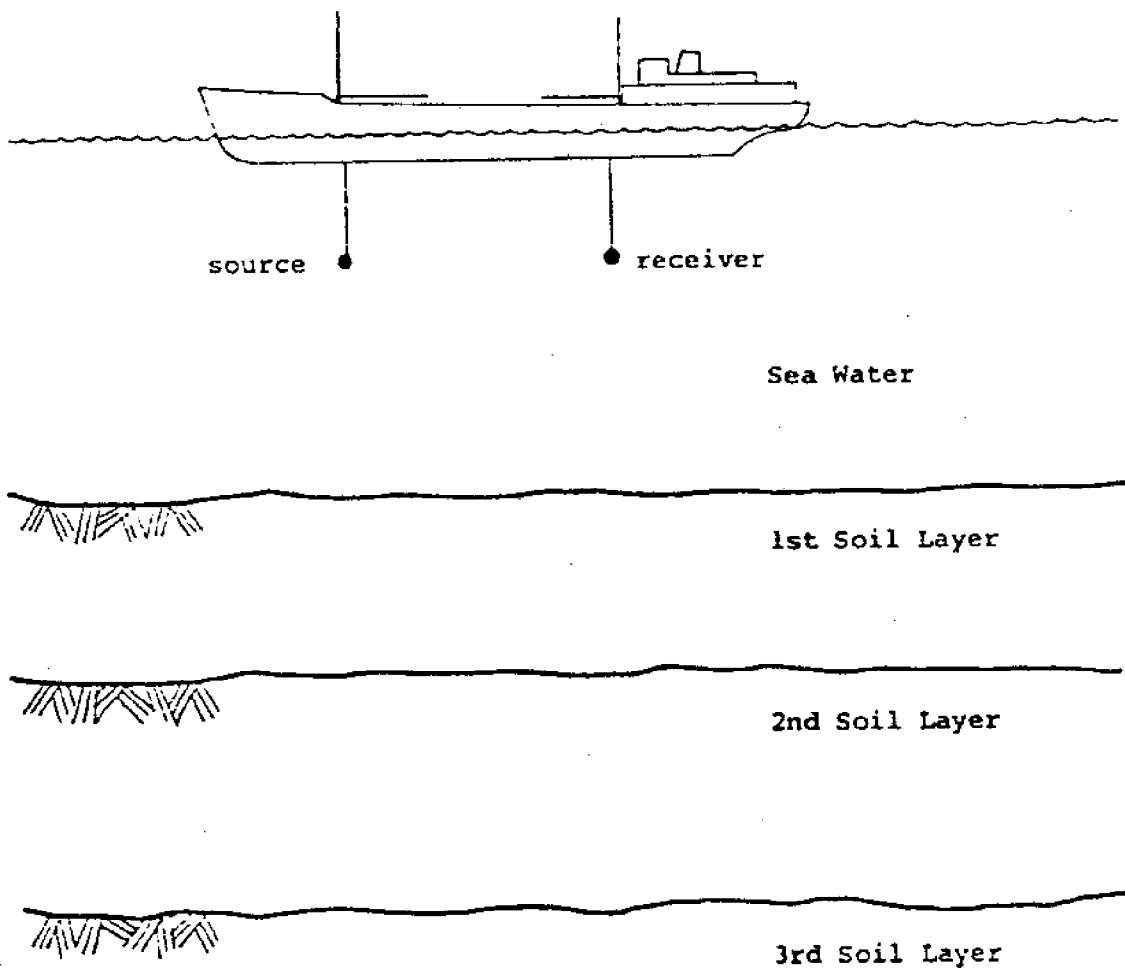


FIGURE 1

REMOTE SEDIMENT CLASSIFICATION DATA ACQUISITION

Figure (1)

Courtesy of Raytheon Company

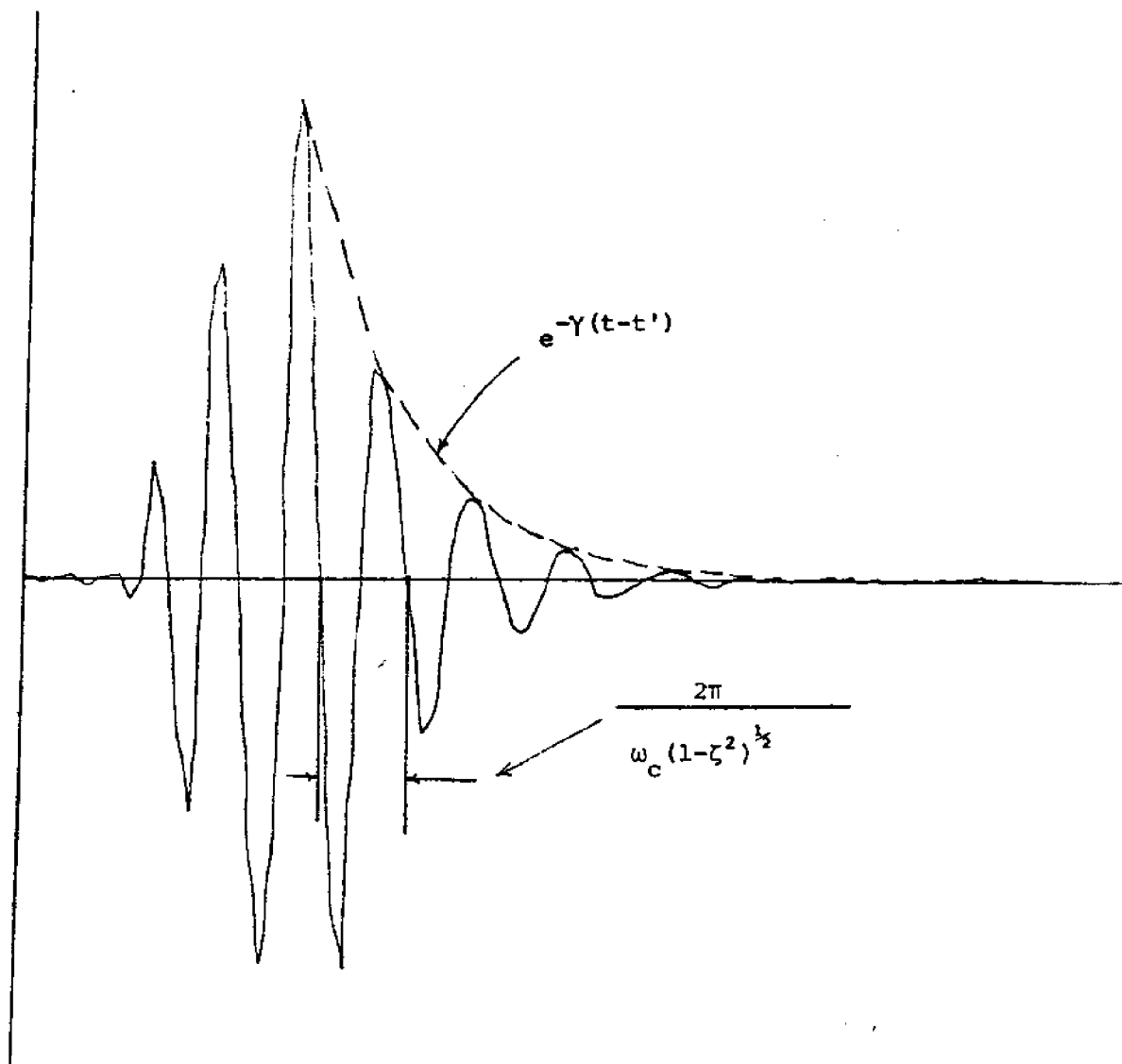


Figure (2)

Time Series of the Return Signal from Ocean

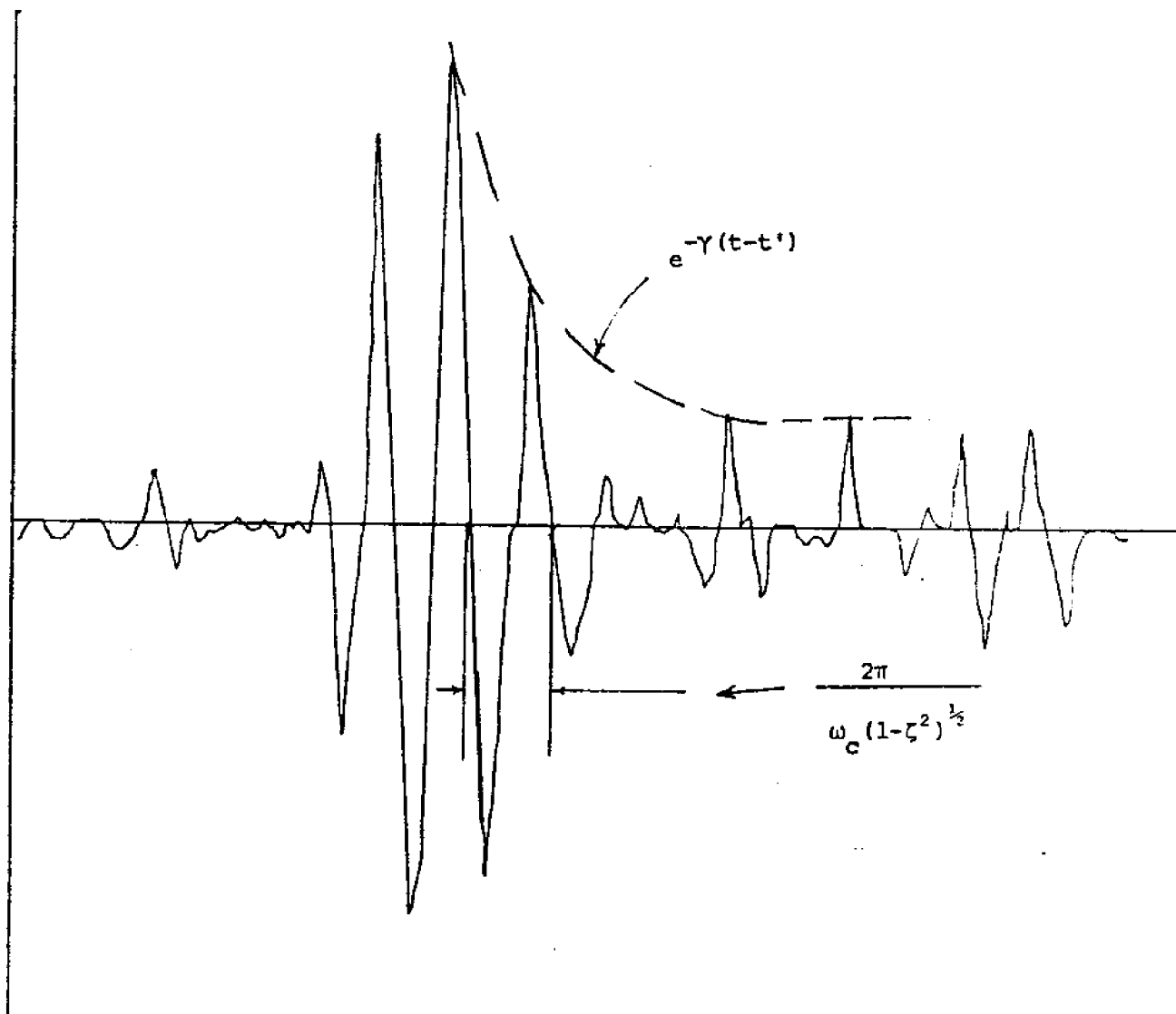


Figure (3)

Time Series of the Return Signal from Ocean Sediments

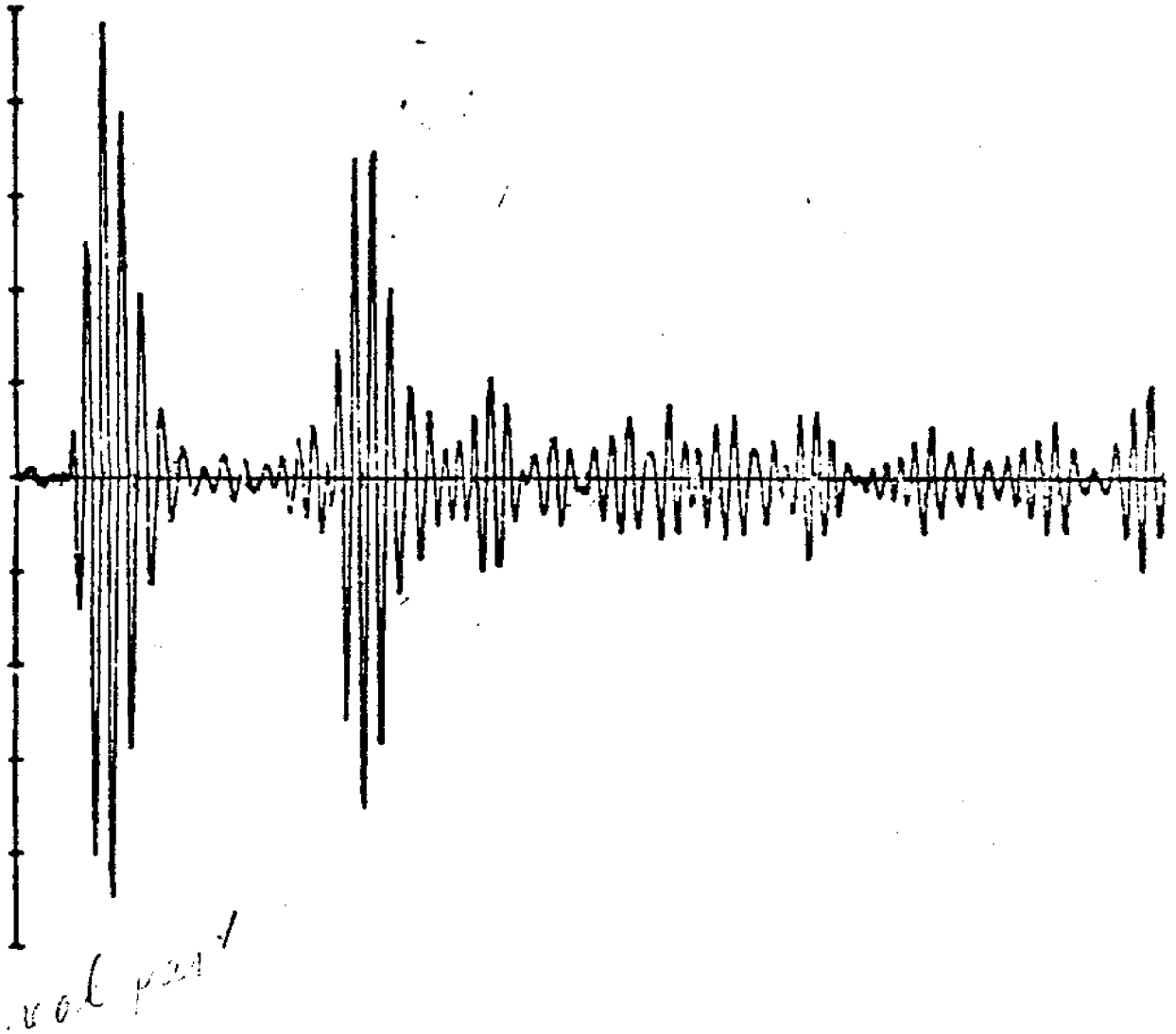


Figure (4)

Time Series of Input and Return Signals

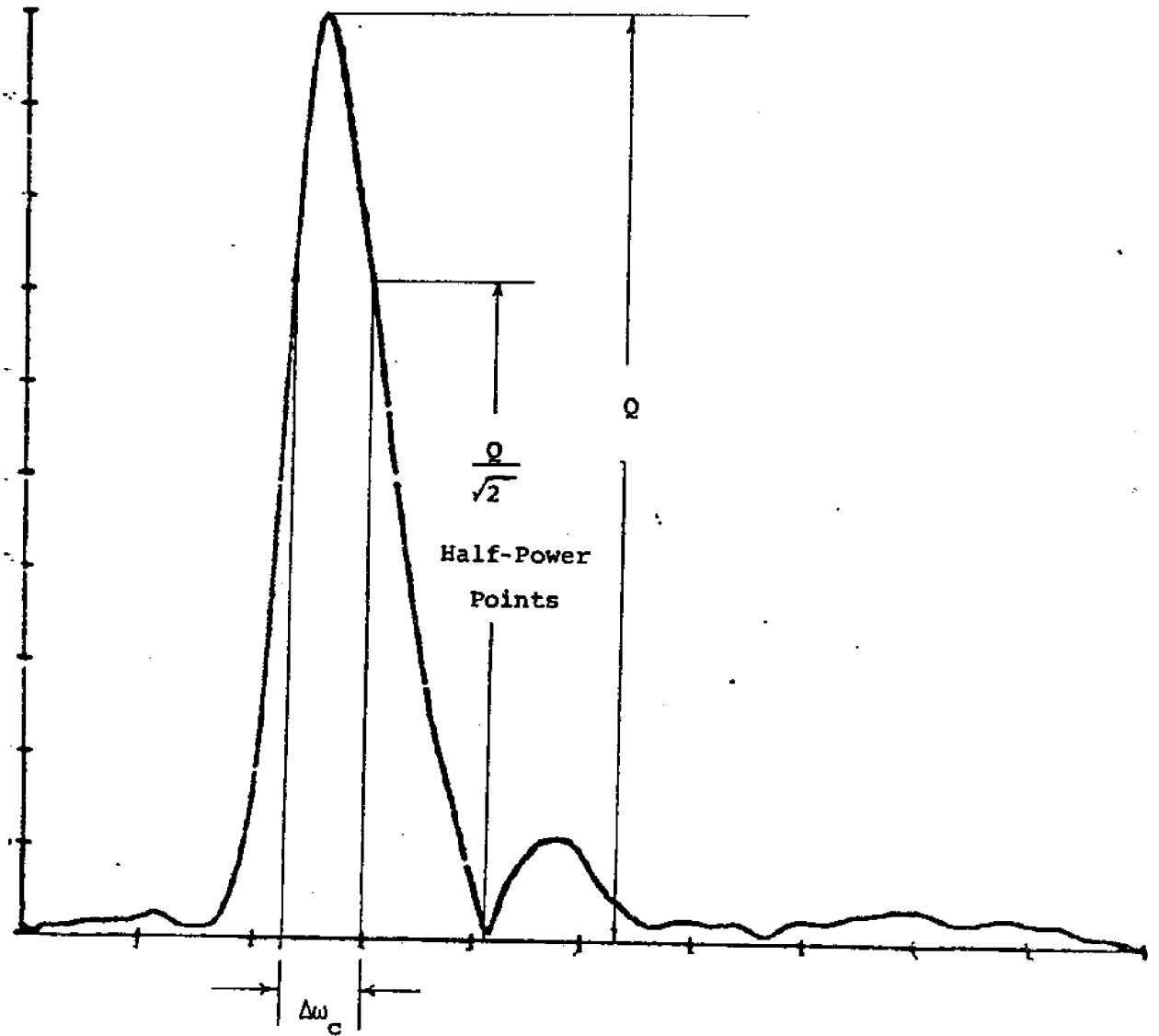


Figure (5)

The Absolute Value of the Transfer Function
Corresponding to Figure (2)

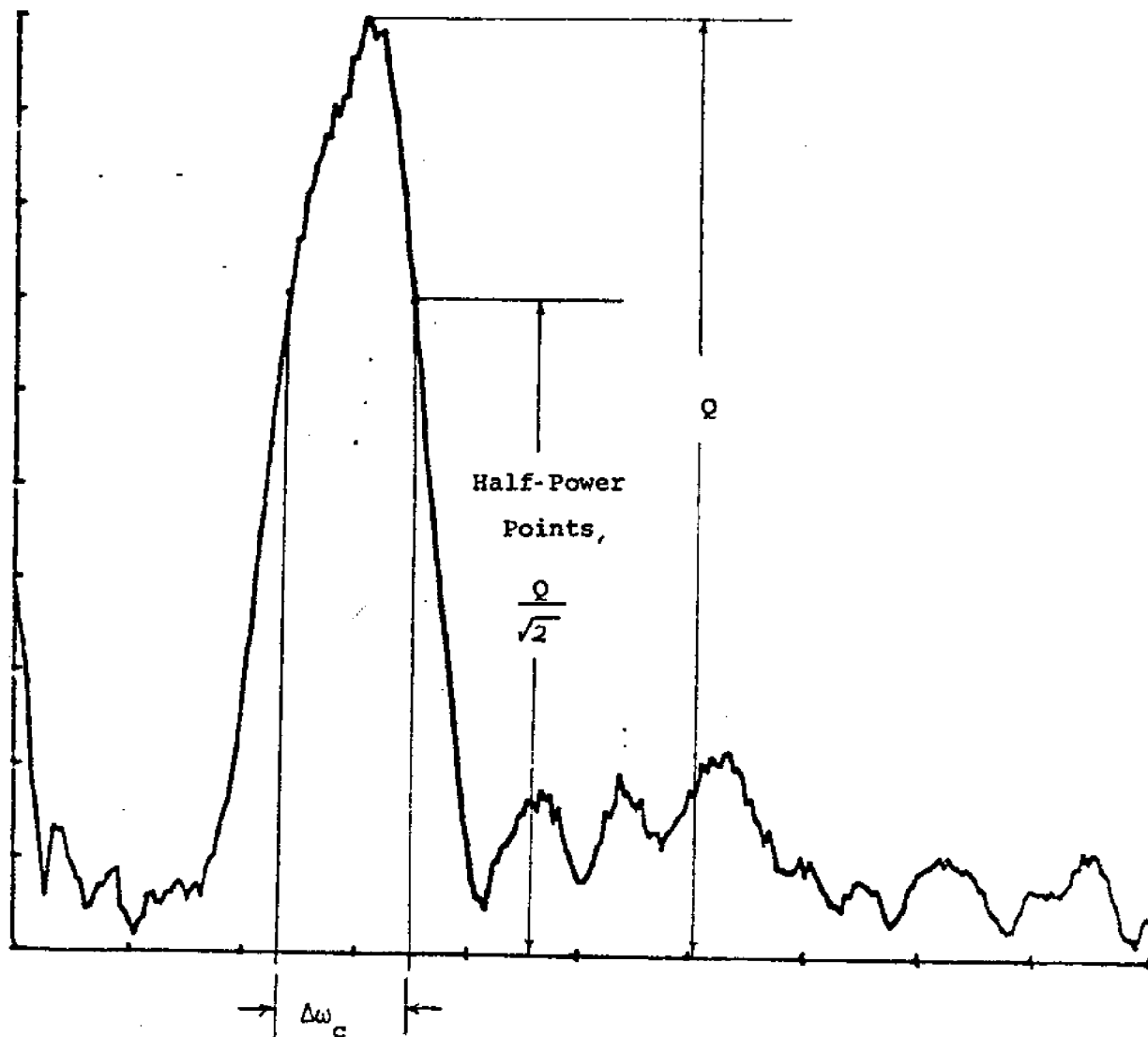


Figure (6)

The Absolute Value of the Transfer Function
Corresponding to Figure (3)

ANALYTICAL MODEL

As indicated in the preceding section, a prototype towed-array measurement system has been employed to provide the data describing soil sediments. It is also noted that the current output is in the form of digital computer print-out, detailing the measured sediment properties in time series representations.

In order to be able to classify the marine sediments remotely, we have to extract the information from the time series indicated by Figures (2) to (4), which represent the return signal from the sediments as well as the input signal excited in the ocean.

It is shown that if the marine sediments are classified according to their physical and engineering properties (i.e., by using a_L = compressional velocity, a_T = shear velocity, ρ = density, γ = attenuation constant, quality factor $Q = \frac{1}{2\zeta}$), then the viscoelastic soil model accurately prescribes the sediment properties which are also obtained through the measurements remotely in the form of the time series representations. This time series representations (measured remotely indicated by Figures (2), (3), and (4)), correspond to analytic models illustrated by Figures (7), (8), provided that we employ viscoelastic soil model of the marine sediments.

Therefore, in the following we shall derive the compressional wave properties of the Green's function in a viscoelastic soil medium.

In a viscoelastic medium, we have the momentum conservation law given as:

$$\partial_t \rho v_i - \partial_j \sigma_{ij} = 0 \quad (1)$$

The macroscopic equation for the stress tensor is given to be

$$\sigma_{ij} = E'_{ijkn} \partial_n u_k + E''_{ijkn} \partial_n \partial_t u_k \quad (2)$$

which relates to the deformation $\partial_{n k} u$. With the aid of these expressions, we obtain

$$\rho \partial_t^2 v_i - E'_{ijkn} \partial_j \partial_n v_k - E''_{ijkn} \partial_j \partial_n \partial_t v_k = 0$$

For simplicity, let us consider transverse displacements, where $\vec{\nabla} \cdot \vec{v}^T = 0$ and for the longitudinal displacements which occur when $\vec{\nabla} \times \vec{v}^L = 0$. Let us take the system to be isotropic such that

$$E'_{ijkn} = \mu' (\delta_{ik} \delta_{jn} + \delta_{in} \delta_{jk} - \frac{2}{3} \delta_{ij} \delta_{kn}) + (\lambda' + \frac{2}{3} \mu') \delta_{ij} \delta_{kn} \quad (3a)$$

$$E''_{ijkn} = \mu'' (\delta_{ik} \delta_{jn} + \delta_{in} \delta_{jk} - \frac{2}{3} \delta_{ij} \delta_{kn}) + (\lambda'' + \frac{2}{3} \mu'') \delta_{ij} \delta_{kn} \quad (3b)$$

We then have

$$\rho \partial_t^2 v_j^T - \mu' \partial_i \partial_i v_j^T - \mu'' \partial_i \partial_i \partial_t v_j^T = 0 \quad (4)$$

In a similar fashion, it can be shown that for longitudinal components

$$\rho \partial_t^2 v_j^L - (\lambda' + 2\mu') \partial_i \partial_i v_j^L - (\lambda'' + 2\mu'') \partial_i \partial_i \partial_t v_j^L = 0 \quad (5)$$

Furthermore, the displacement equation for the visco-elastic medium with a forcing term \vec{f} can be written as

$$\rho \partial_t^2 \vec{u} - [(\lambda' + \mu') + (\lambda'' + \mu'')] \partial_t \vec{\nabla} (\vec{\nabla} \cdot \vec{u}) - (\mu' + \mu'') \nabla^2 \vec{u} = \rho \vec{f} \quad (6)$$

Taking the divergence of (6), we obtain

$$\rho \partial_t^2 \vec{\nabla} \cdot \vec{u} - [(\lambda' + 2\mu') + (\lambda'' + 2\mu'')] \partial_t \nabla^2 (\vec{\nabla} \cdot \vec{u}) = \rho \vec{\nabla} \cdot \vec{f} \quad (7)$$

Defining $\vec{\nabla} \cdot \vec{u} = X$, Equation (7) becomes

$$\partial_t^2 X - \frac{(\lambda' + 2\mu')}{\rho} \nabla^2 X - \frac{(\lambda'' + 2\mu'')}{\rho} \partial_t \nabla^2 X = \vec{\nabla} \cdot \vec{f} \quad (8)$$

Hence, the appropriate Green's function for $\vec{\nabla} \cdot \vec{u} = X$ or $\vec{\nabla} \cdot \vec{v} = \dot{X}$ can be written as

$$[\partial_t^2 - \frac{(\lambda' + 2\mu')}{\rho} \nabla^2 - \frac{(\lambda'' + 2\mu'')}{\rho} \nabla^2 \partial_t] \tilde{g}(t-t'; \vec{r}-\vec{r}') = \delta(\vec{r}-\vec{r}') \delta(t-t') \quad (9)$$

It is often more convenient to discuss and practical, both in this specific model and in general, to use the spatial Fourier transform of the Green's function in Equation (9). Thus,

$$\tilde{g}(t-t'; \vec{r}-\vec{r}') = \iiint \frac{d^3k}{(2\pi)^3} e^{-i\vec{k} \cdot (\vec{r}-\vec{r}')} g(t-t'; k, \lambda, \mu) \quad (10a)$$

The employment of the relationship

$$\delta(\vec{r}-\vec{r}') = \iiint \frac{d^3k}{(2\pi)^3} e^{-i\vec{k} \cdot (\vec{r}-\vec{r}')} \quad (10b)$$

reduces Equation (9) to

$$[\partial_t^2 + \frac{(\lambda' + 2\mu')}{\rho} k^2 + \frac{(\lambda'' + 2\mu'')}{\rho} k^2 \partial_t] g(t-t'; k, \lambda, \mu) = \delta(t-t') \quad (11)$$

The above relationships state that in this example $\tilde{g}(t-t'; \vec{r}-\vec{r}')$ is the Green's function for the ordinary differential equation describing the non-equilibrium

behavior. Specifically, it gives the response to a unit impulsive external force at time t' . Both $\vec{\nabla} \cdot \vec{u}$ for a general external disturbance and $g(t-t'; k, \lambda, \mu)$ is called the retarded Green's function.

It is now appropriate to discuss the Fourier transform of $g(t-t'; k, \lambda, \mu)$. Upon transformation, we then have

$$g(t-t'; k, \lambda, \mu) = \int_{-\infty}^{\infty} \frac{d\omega}{2\pi} e^{-i\omega(t-t')} g(\omega; k, \lambda, \mu) \quad (12)$$

and

$$g(\omega; k, \lambda, \mu) = \int_{-\infty}^{\infty} d(t-t') e^{-i\omega(t-t')} g(t-t'; k, \lambda, \mu) \quad (13)$$

$$= \int_0^{\infty} d(t-t') e^{-i\omega(t-t')} g(t-t'; k, \lambda, \mu)$$

where the last transformation reflects, that is the causal, nature of $g(t-t'; k, \lambda, \mu)$. It is also convenient to define $g(\omega + i\epsilon; k, \lambda, \mu)$ which is a function of complex variable $z = \omega \pm i\epsilon$, for z in either lower or upper half complex plane according to the choice of the sign of the exponential. It should be further noted that the last integral in Equation (13) provides such a definition since it is well defined and exponentially decreasing when $\omega \rightarrow z = \omega \pm i\delta$ ($\delta > 0$). The function of a complex variable z , $g(z; k, \lambda, \mu) \rightarrow g(\omega; k, \lambda, \mu)$ as $\delta \rightarrow 0$, is clearly analytic and bounded in the defined lower or upper half z plane. By the inspection of Equation (11), $g(z; k, \lambda, \mu)$ satisfies

$$\left(-z^2 + \frac{(\lambda' + 2\mu')}{\rho} k^2 + iz \frac{(\lambda'' + 2\mu'')}{\rho} k^2 \right) g(z; k, \lambda, \mu) = 1 \quad (14)$$

By the inversion of Equation (14), we can write

$$g(t-t'; k, \lambda, \mu) = \int_{-\infty}^{\infty} \frac{d\omega}{2\pi} \frac{e^{i\omega(t-t')}}{[-\omega^2 + (\lambda' + 2\mu')k^2/\rho + i\omega(\lambda'' + 2\mu'')k^2/\rho]}$$
(15)

where the integration is along the real axis or any path from $-\infty$ to ∞ in the upper half plane.

Explicitly, the impulse function is given to be

$$g(t-t'; k, \lambda, \mu) = \eta(t-t') e^{-(t-t')(\lambda'' + 2\mu'')k^2/2\rho} \cdot \frac{\sin[(t-t')k \frac{(\lambda' + 2\mu')^{1/2}}{\rho} (1 - \frac{k^2 \ell^2}{\rho})^{1/2}]}{k [\frac{(\lambda' + 2\mu')}{\rho}]^{1/2} (1 - \frac{k^2 \ell^2}{\rho})^{1/2}}$$
(16)

where $\ell^2 = \frac{(\lambda'' + 2\mu'')^2}{4(\lambda' + 2\mu')}$ and $\eta(t-t') = 1$ when $t > t'$ and 0 when $t < t'$.

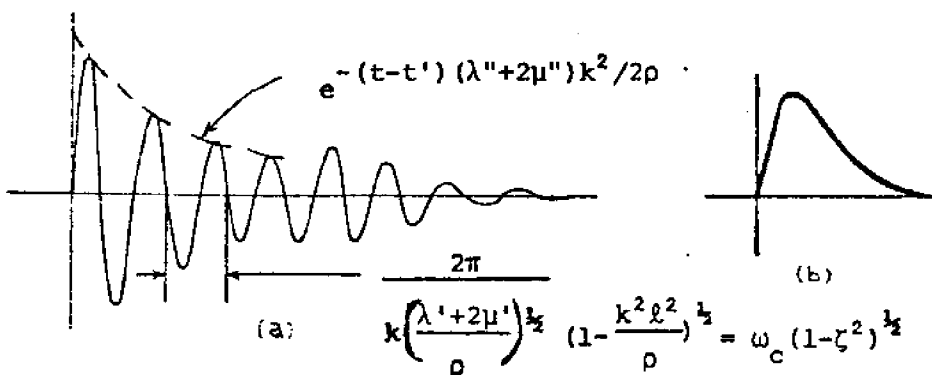


Figure (7): The retarded response, $g(t-t'; k, \lambda, \mu)$

(a) Underdamped case when $2(\lambda' + 2\mu') > \lambda'' + 2\mu''$

(b) Overdamped case when $2(\lambda' + 2\mu') < \lambda'' + 2\mu''$

For real ω , the Green's function, $g(\omega; k, \lambda, \mu)$ is usually divided into two parts: a dissipative part and a reactive part. In this case, and more generally when the system is stationary, that is time reversal invariant, these are given respectively by the imaginary and real parts of $g(\omega; k, \lambda, \mu)$, and are denoted as $g''(\omega; k, \lambda, \mu)$ and $g'(\omega; k, \lambda, \mu)$:

$$g''(\omega; k, \lambda, \mu) = \frac{-[(\lambda'' + 2\mu'')k^2/\rho]\omega}{[k^2(\frac{\lambda' + 2\mu'}{\rho}) - \omega^2]^2 + [\omega(\frac{\lambda'' + 2\mu''}{\rho})k^2]^2} \quad (17a)$$

$$g'(\omega; k, \lambda, \mu) = \frac{(\lambda' + 2\mu')k^2/\rho - \omega^2}{[k^2(\frac{\lambda' + 2\mu'}{\rho}) - \omega^2]^2 + [\omega(\frac{\lambda'' + 2\mu''}{\rho})k^2]^2} \quad (17b)$$

The Fourier transform of Equation (17a), is the imaginary odd function of time as illustrated in Figure (8a). Hence, we have

$$g''(t-t'; k, \lambda, \mu) = \int_{-\infty}^{\infty} \frac{d\omega}{2\pi} g''(\omega; k, \lambda, \mu) e^{\pm i\omega(t-t')} \quad (18a)$$

$$= -ie^{-(t-t')} (\lambda'' + 2\mu'')k^2/2\rho \frac{\sin[(t-t')k(\lambda' + 2\mu')^{1/2}/\rho^{1/2}(1-k^2\ell^2/\rho)^{1/2}]}{2k(\frac{\lambda' + 2\mu'}{\rho})^{1/2} (1 - \frac{k^2\ell^2}{\rho})^{1/2}}$$

Likewise, the Fourier transform of Equation (17b) is the real even function of time as illustrated in Figure (8b)

$$\begin{aligned}
 g'(t-t'; k, \lambda, \mu) &= \frac{1}{2} [g(t-t'; k, \lambda, \mu) + g(t'-t; k, \lambda, \mu)] \\
 &= e^{-(t-t')(\lambda'' + 2\mu'')k^2/2\rho} \frac{\sin[(t-t')k(\lambda' + 2\mu')^{1/2}/\rho^{1/2} (1-k^2\ell^2/\rho)^{1/2}]}{k(\frac{\lambda' + 2\mu'}{\rho})^{1/2} (1-\frac{k^2\ell^2}{\rho})^{1/2}}
 \end{aligned}
 \tag{18b}$$

It is noted that

$$g(\omega; k, \lambda, \mu) = \frac{\rho}{(\lambda' + 2\mu')k^2} H(\omega; k, \lambda, \mu)
 \tag{19}$$

Thus, $h(t-t'; k, \lambda, \mu)$ differs from $g(t-t'; k, \lambda, \mu)$ by a factor of $(\lambda' + 2\mu')k^2/\rho$ according to the relationship indicated by Equation (19).

Since the response is causal, or equivalently, since $g(z; k, \lambda, \mu)$ which we have defined to be analytic in the upper or lower half plane, the real and imaginary parts of $g(\omega; k, \lambda, \mu)$ are related by Hilbert transform according to the relations

$$g'(\omega; k, \lambda, \mu) = P \int_{-\infty}^{\infty} \frac{d\omega'}{\pi} \frac{g''(\omega; k, \lambda, \mu)}{\omega' - \omega}
 \tag{20a}$$

$$g''(\omega; k, \lambda, \mu) = -P \int_{-\infty}^{\infty} \frac{d\omega'}{\pi} \frac{g'(\omega; k, \lambda, \mu)}{\omega' - \omega}
 \tag{20b}$$

where "P" implies principal value integral, that is, an integral symmetrical about the singularity.

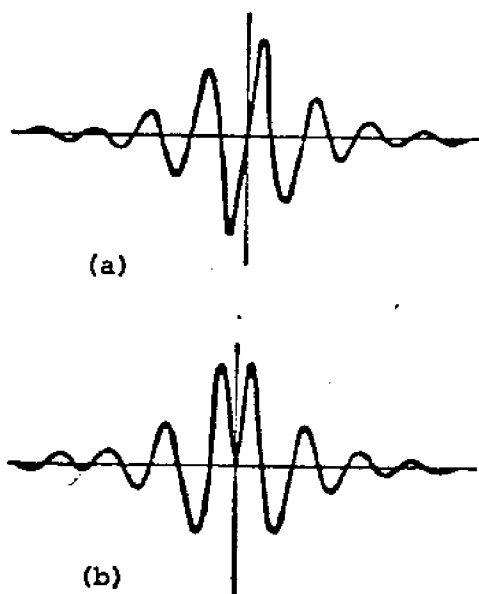


Figure (8): (a) Purely imaginary absorptive response
(b) The dispersive response of underdamped oscillation in the time domain

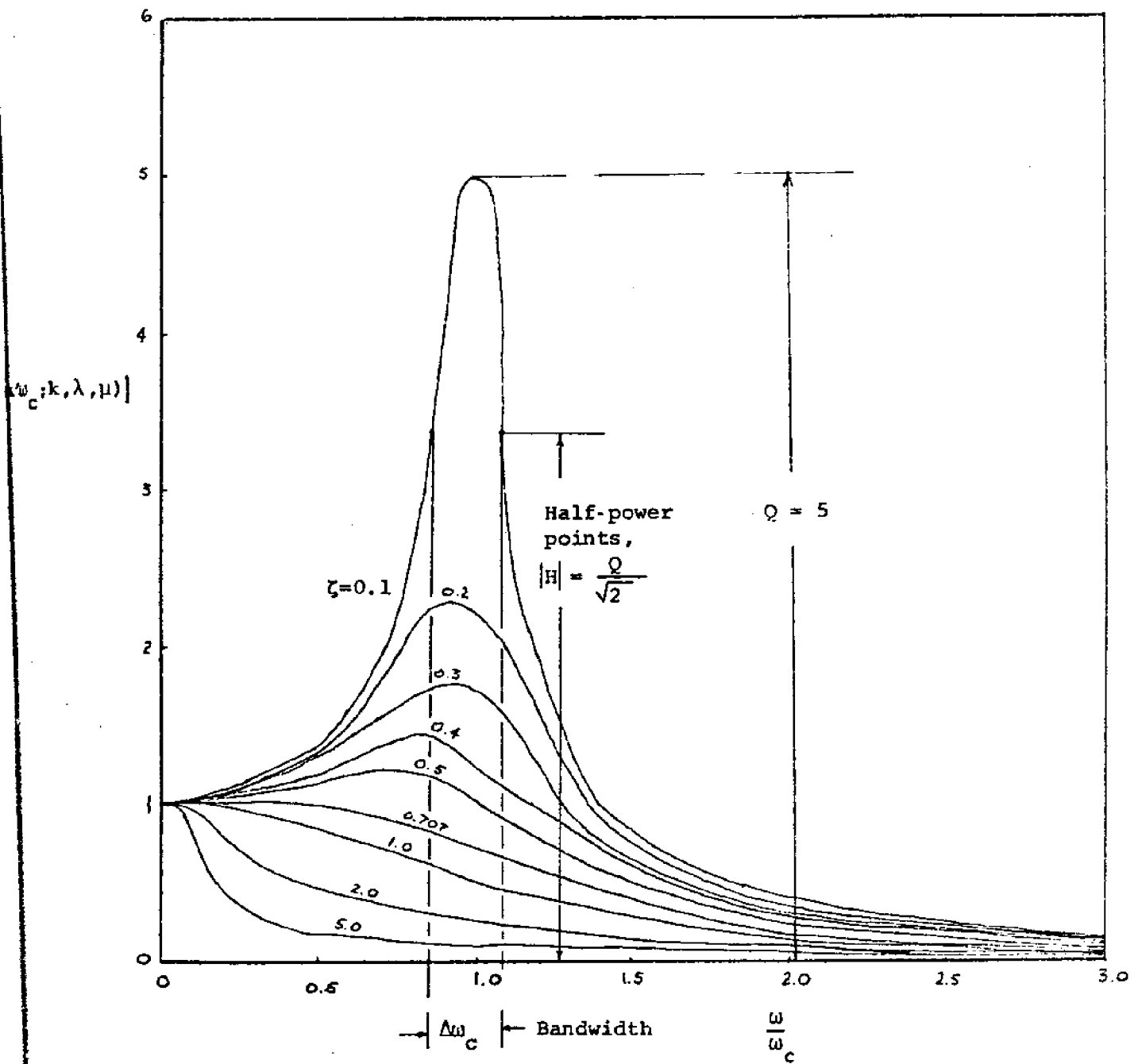


Figure (9): Frequency response of compressional wave system

$$\omega_c = k \frac{(\lambda' + 2\mu')^{1/2}}{\rho^{1/2}} \quad \zeta = \frac{(\lambda'' + 2\mu'')k}{2(\lambda' + 2\mu')^{1/2} \rho^{1/2}} \quad Q = \frac{1}{2\zeta}$$

The transfer function for the compressional system parameters of the visco-elastic soil is given by Equation (19):

$$H(\omega; k, \lambda, \mu) = \frac{1}{1 - \frac{\omega^2 \rho}{(\lambda' + 2\mu') k^2} + i\omega \frac{(\lambda'' + 2\mu'') k^2}{\rho}} \quad (20)$$

where the complex number $H(\omega; k, \lambda, \mu)$ contains the phase lag between excitation and response, the response/excitation amplitude ratio $|H|$. For signal processing purpose it is convenient to redefine the excitation in such a way that $|H(0; k, \lambda, \mu)| = 1$. In Fig. (9), the magnitude of this normalized frequency response is sketched. In this plot, another measure of attenuation is shown, the quality factor Q , which in this case measures $|H(0; k, \lambda, \mu)|$ when

$$\frac{\omega_c^2}{c} = \left(\frac{\lambda' + 2\mu'}{\rho}\right) k^2, \quad Q = 1/2\zeta = \frac{[(\lambda' + 2\mu')\rho]^{1/2}}{(\lambda'' + 2\mu'') k} \quad (21)$$

Also of importance is the "bandwidth" of the resonance peak, particularly for the case of light damping, say $Q \geq 10$. In this case $|H(0; k, \lambda, \mu)|$ is nearly a maximum at $\omega = \left(\frac{\lambda' + 2\mu'}{\rho}\right)^{1/2} k$ and is nearly symmetric about $\left(\frac{\lambda' + 2\mu'}{\rho}\right)^{1/2} k$. The half-power points are points for which $|H(0; k, \lambda, \mu)| = Q/\sqrt{2}$. For light damping the attenuation constant is small, and the half power points are given approximately by $\omega = \left(\frac{\lambda' + 2\mu'}{\rho}\right) k(1 \pm \zeta)$ or $\omega = \left(\frac{\lambda' + 2\mu'}{\rho}\right) k(1 \pm 1/2Q)$, and this frequency spread is often used as a measure of the system bandwidth. In a subsequent paper it is necessary to measure power spectra. For this purpose we shall use a shaping filter that responds primarily to frequencies in a narrow band which can be used to measure power density spectra. Mean square fluctuations of $X = \vec{\nabla} \cdot \vec{u}$ can be manipulated to yield involving compressional wave spectrum

(16)

$$P_o = \left(\frac{2\zeta}{\pi}\right) \left(\frac{\lambda'+2\mu'}{\rho}\right)^{\frac{3}{2}} k^3 E[X^2] = \frac{1}{\pi Q} \left(\frac{\lambda'+2\mu'}{\rho}\right)^{\frac{3}{2}} k^3 \lim_{T \rightarrow \infty} \frac{1}{T} \int_0^T X^2(t) dt \quad (22)$$

For this result to be useful, Q must be sufficiently large for the bandwidth of the filter to be narrow enough for the purpose at hand (see Fig. (9)). It⁽²⁾ is shown that the mean square response of a lightly damped system filter is determined mainly by the input spectrum at those frequencies within the filter bandwidth. Thus, P_o in Eq. (22) can be interpreted as an average of $P(\omega)$ over the filter bandwidth

$$k \left(\frac{\lambda'+2\mu'}{\rho}\right)^{\frac{1}{2}} (1-\zeta) < k \left(\frac{\lambda'+2\mu'}{\rho}\right)^{\frac{1}{2}} (1+\zeta) \quad (23)$$

use of Eq. (22) with finite T involves the problem of statistical estimation. The more the Q of the filter is increased in order to measure detail in $P_f(\omega)$, the longer T must be to achieve a reliable measurement. This problem is studied in some detail in a subsequent paper⁽¹⁾.

Compressional Wave System of a Visco-Elastic Soil As A Narrow Band Gaussian Process.

It is noted from the actual data, see Figure (3) which is provided by the Raytheon Company where compressional wave system represents lightly damped system. The appearance of such processes (see Fig. 4) leads to the representation as a sinusoidal wave with a randomly varying amplitude and phase.

When the process bandwidth is not infinitely narrow, it is of interest to find the expected compressional frequency $\omega_c = k \left(\frac{\lambda'+2\mu'}{\rho}\right)^{\frac{1}{2}}$, so that the expected number of cycles, as shown in Fig. (4) can be computed. The result of this type of calculation was done by Rice in his classic paper⁽³⁾:

$$\left(\frac{\lambda'+2\mu'}{\rho} k^2\right) = \frac{\int_{-\infty}^{\infty} \omega^2 P_{XX}(\omega; k, \lambda, \mu) d\omega}{\int_{-\infty}^{\infty} P_{XX}(\omega; k, \lambda, \mu) d\omega} = -\frac{R''_{XX}(0; k, \lambda, \mu)}{R_{XX}(0; k, \lambda, \mu)} = \frac{\sigma_X^2}{\sigma_X^2} \quad (24)$$

where P_{XX} is power density spectrum, R_{XX} auto correlation function and σ_X^2 variance of X . The expected frequency $\omega_c = \left(\frac{\lambda'+2\mu'}{\rho}\right)^{1/2} k$ is just $2\pi f_c^+$, where f_c^+ is the expected number of upward crossings of the line $X=0$ because of the way a cycle is defined in Fig. (4). The notion of a cycle loses significance if the process is not narrow band. It can also be shown, using Equation (24), that if a highly resonant single-degree of freedom system is excited by white Gaussian noise, the expected frequency ω_c is just the undamped natural frequency of the system ω_c . This result is approximately true as long as the spectrum of the excitation is relatively flat over the bandwidth of the system and does not have strong peaks at other frequencies near the system resonant frequencies.

App 111

SOIL IDENTIFICATION PROBLEM BY REMOTE ACOUSTIC SENSING

I - Parameters obtainable from statistical signal processing techniques.

- (a) ω_n = natural frequency of subbottom soil;
- (b) ω_d = damped natural frequency of subbottom soil;
- (c) γ = attenuation coefficient;
- (d) Q = quality (damping) factor of subbottom soil.

II - Parameters obtainable from normal and oblique incident techniques.

- (a) a_L = compressional wave velocity of subbottom soil;
- (b) a_T = shear wave velocity of subbottom soil.

III - From the above measurements we obtain information about

$\lambda', \lambda'', \mu', \mu'', \rho,$ and k (which is a Fourier transform parameter).

Definition of Symbols in Terms of Soil Parameters

Shear Parameters

$$\zeta = \frac{\mu'' k}{2(\mu' \rho)^{1/2}} ;$$

$$\omega_n = k(\mu' / \rho)^{1/2} ;$$

$$\zeta \omega_n = \frac{\mu'' k^2}{2\rho} ;$$

$$\omega_n (1-\zeta^2)^{1/2} = k(\mu' / \rho)^{1/2} \left(1 - \frac{\mu''^2 k^2}{4\mu' \rho}\right)^{1/2} ;$$

$$h(t) = \frac{\omega_n e^{-\zeta \omega_n t} \sin[\omega_n (1-\zeta^2)^{1/2} t]}{(1-\zeta^2)^{1/2}} ;$$

$$h(t) = \frac{k \left(\frac{\mu'}{\rho}\right)^{1/2} e^{-\frac{\mu'' k^2 t}{2\rho}} \sin\left[k \left(\frac{\mu'}{\rho}\right)^{1/2} \left(1 - \frac{\mu''^2 k^2}{4\mu' \rho}\right)^{1/2} t\right]}{\left(1 - \frac{\mu''^2 k^2}{4\mu' \rho}\right)^{1/2}}$$

Compressional Parameters

$$\zeta = \frac{(\lambda'' + 2\mu'') k}{2[(\lambda' + 2\mu') \rho]^{1/2}} ;$$

$$\omega_n = k(\lambda' + 2\mu' / \rho)^{1/2}$$

$$\zeta \omega_n = \frac{k^2 (\lambda'' + 2\mu'')}{2\rho} ;$$

$$\omega_n (1-\zeta^2)^{1/2} = k \left(\frac{\lambda' + 2\mu'}{\rho}\right)^{1/2} \left(1 - \frac{(\lambda'' + 2\mu'')^2 k^2}{4(\lambda' + 2\mu') \rho}\right)^{1/2}$$

$$h(t) = \frac{\omega_n e^{-\zeta \omega_n t} \sin[\omega_n (1-\zeta^2)^{1/2} t]}{(1-\zeta^2)^{1/2}}$$

$$h(t) = \frac{k \left(\frac{\lambda' + 2\mu'}{\rho}\right)^{1/2} e^{-\frac{(\lambda'' + 2\mu'') k^2 t}{2\rho}} \sin\left[k \left(\frac{\lambda' + 2\mu'}{\rho}\right)^{1/2} \left(1 - \frac{(\lambda'' + 2\mu'')^2 k^2}{4(\lambda' + 2\mu') \rho}\right)^{1/2} t\right]}{\left(1 - \frac{(\lambda'' + 2\mu'')^2 k^2}{4(\lambda' + 2\mu') \rho}\right)^{1/2}}$$

Definition of Symbols in Terms of Soil Parameters (cont'd)

ρ = density of soil

k = Fourier transform parameter

μ' = shear modulus (real part of shear parameter)

μ'' = shear viscosity (imaginary part of shear parameter)

λ' = real part of compressional parameter

λ'' = imaginary part of the compressional parameter

I - (a) Natural Frequency of Subbottom Soil -

In frequency domain we can define

$$\rho(\omega; k, \mu, \lambda) = \int_{-\infty}^{\infty} dt e^{i\omega t} \langle r(t; k, \mu, \lambda) r(t+\tau; k, \mu, \lambda) \rangle$$

where $\langle r(t; k, \mu, \lambda) r(t+\tau; k, \mu, \lambda) \rangle$ is the autocorrelation function of the compressional wave system response $r(t; k, \mu, \lambda)$.

For a stationary random process with zero mean, the statistical average frequency or expected frequency is where

$$\omega_n = \left[\frac{\int_{-\infty}^{\infty} \rho(\omega; k, \mu, \lambda) \omega^2 d\omega}{\int_{-\infty}^{\infty} \rho(\omega; k, \mu, \lambda) d\omega} \right]^{1/2} \quad (1)$$

The result can be simply stated and has a simple interpretation; i.e. ω_n is simply a weighted average of ω^2 in which $P(\omega; k, \mu, \lambda)$ is the weighting function. We give a brief outline of the above expression.

Let $u(t)$ be a stationary process and let f_a^+ be the expected frequency of crossing the level $u=a$ with positive slope. It will be seen that for a narrow band process f_a^+ is just the expected frequency of cycles so that $\omega_n = 2\pi f_a^+$. It is more difficult to consider a general value of a at this point and set $a=0$ at the end. Later on, use will be made of f_a^+ .

We next consider the geometry involved in a sample function crossing the level $u=a$ during a particular small time interval dt . The situation is sketched in Fig. (1). All sample functions cross the line $t=t$ but only a small fraction of these cross the line $x=a$ with positive slope $\dot{u} > 0$ during the interval dt . Two such samples are indicated in the figure. We suppose that dt is so small that the samples can be treated as straight lines in the interval. If a sample crosses $t=t$ with an u value less than a , then it will also cross $u=a$ with a positive slope during the time dt if its slope \dot{x} at $t=t$ has any value from ∞ down to the limiting value $(a-u)/dt$. Using

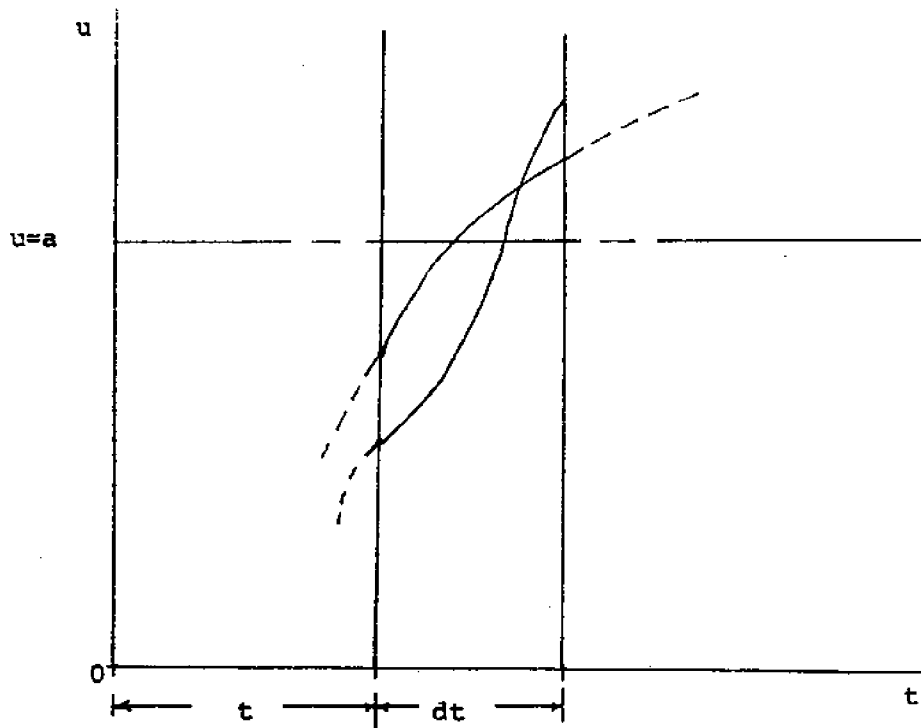


Figure (1): Sample functions which cross $u=a$ during the interval dt have certain restrictions on the combination of values $u(t)$ and $\dot{u}(t)$ taken on at the beginning of the interval.

this statement we can examine each sample at $t=t$ and decide whether or not its combination u and \dot{u} values will yield a crossing of $u=a$.

An analytic method of examining combinations of u and \dot{u} values is provided by the joint probability distribution of u and \dot{u} for this stationary process. This distribution can be described by a joint density function $p(u, \dot{u})$ which would be somewhat similar to that sketched in Figure (2). The probability of a sample having u between u and $u+du$ and having \dot{u} between \dot{u} and $\dot{u}+d\dot{u}$ is $p(\dot{u}, u)d\dot{u}du$. In the (u, \dot{u}) plane the "favorable" combinations of u and \dot{u} values (i.e. those that cause crossings of $u=a$ with positive slope in Figure (1).) are shown in the shaded area of Figure (2) between the line $u=a$ and the line where \dot{u} equals the limiting value $(a-u)/dt$.

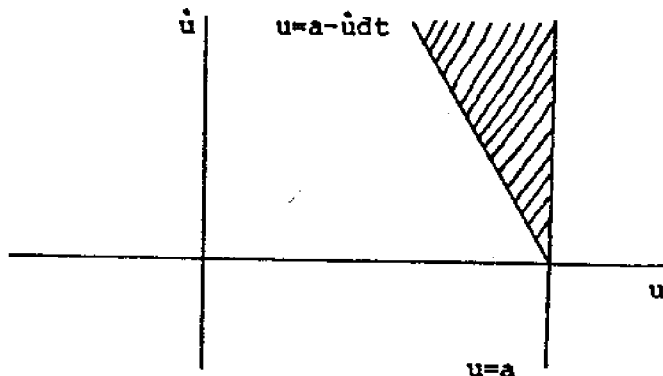


Figure (2)

Now the expected number of crossings of $u=a$ during dt is just the same as the fraction of "favorable" combination out of all possible combinations, since a favorable combination gives no crossing. Finally, if we divide by dt we get the expected number of such crossings per unit time, f_a^+ . Writing this out, we have

$$f_a^+ = \frac{1}{dt} \int_0^{\infty} d\dot{u} \int_{a-\dot{u}dt}^{\infty} p(u, \dot{u}) du$$

where the integration limits have been chosen to cover the shaded area in Figure (2). For small dt the u variable is substantially equal to a in the u integration so that we have, on letting $dt \rightarrow 0$,

$$f_a^+ = \int u(a, u) du \quad (2)$$

This result for the expected number of crossings of the level $u=a$, with positive slope, per unit time, applies to any stationary process not necessarily normal and not necessarily narrow-band. It should be noted that f_a^+ is an ensemble average in the sense that it is based on the fraction of "favorable" ensemble members taken at a fixed instant of time. Because the process is stationary f_a^+ is independent time, i.e., the average frequency of crossing level $u=a$ is constant. This does not imply that along a particular sample function the time-average frequency of crossing of $u=a$ will be equal to f_a^+ unless the process is ergodic.

In order to evaluate Equation (2) we now make the assumption that $u(t)$ is a stationary normal or Gaussian process with zero mean. This requires that the joint density take the following form:

$$p(u, \dot{u}) = \frac{1}{2\pi\sigma_u\sigma_{\dot{u}}} e^{-\frac{1}{2}\left(\frac{u^2}{\sigma_u^2} + \frac{\dot{u}^2}{\sigma_{\dot{u}}^2}\right)} \quad (3)$$

Note that Equation (3) implies that u and \dot{u} are uncorrelated. Substituting in Equation (2) and evaluating the integral we find

$$f_a^+ = \frac{1}{2\pi} \frac{\sigma_{\dot{u}}}{\sigma_u} e^{-\frac{a^2}{2\sigma_u^2}} \quad (4)$$

The quantities σ_u and $\sigma_{\dot{u}}$ are obtained from the spectral density $P(\omega; k, \mu, \lambda)$ or auto correlation function $R(\tau)$, i.e.

$$\sigma_u^2 = \int_{-\infty}^{\infty} P(\omega; k, \mu, \lambda) d\omega = R(0) \quad (5)$$

$$\sigma_u^2 = \int_{-\infty}^{\infty} \omega^2 P(\omega; k, \mu, \lambda) d\omega = R''(0)$$

Hence, in Equation (1) we also have

$$\omega_n = \frac{\sigma_u^2}{\sigma_u^2} = - \frac{R''(0)}{R(0)}$$

Returning to our original problem, we set $a=0$ in Equation (4) to obtain the expected frequency, in crossing per unit time, of zero crossings with positive slope. Finally, if the process is narrow-band the probability is very high that each such crossing implies a complete "cycle" and thus the expected frequency, in cycles per unit time, is f_0^+ . The result in Equation (1) follows from Equation (4) and (6) on setting $a=0$. It should be emphasized that this result is restricted to normal process with zero mean. Hence, we can determine the natural frequency of our compressional wave system ω_n . In soil parameters,

$$\omega_n = k \left[\frac{(\lambda' + 2\mu')}{\rho} \right]^{\frac{1}{2}}$$

I - (b) Damped Natural Frequency of Subbottom Soil - $\omega_d = \omega_n (1 - \zeta^2)^{1/2}$

The compressional wave system response is of the form in time domain

$$r(t) = A_0 e^{-(\zeta\omega_n)t} \sin(\omega_n (1 - \zeta^2)^{1/2} t)$$

where

A_0 = initial value of the amplitude

$\zeta\omega_n$ = system attenuation constant

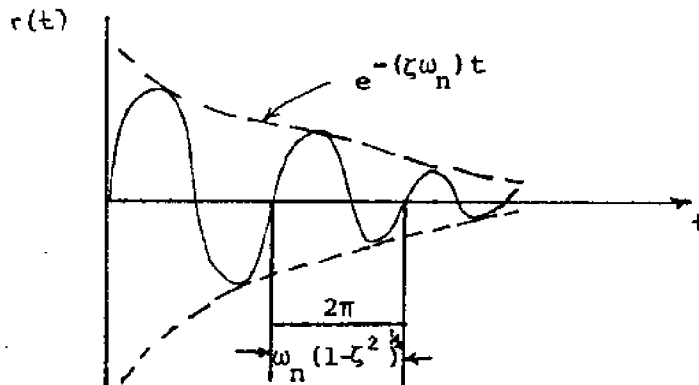
$\omega_n (1 - \zeta^2)^{1/2}$ = damped frequency of the system

in terms of soil parameters

$$\omega_n (1 - \zeta^2)^{1/2} = k [(\lambda' + 2\mu') / \rho]^{1/2} \left[1 - \frac{(\lambda'' + 2\mu'')^2 k^2}{4\rho(\lambda' + 2\mu')} \right]^{1/2}$$

$$\zeta\omega_n = \frac{k^2 (\lambda'' + 2\mu'')}{2\rho}$$

which is sketched below



Response of lightly damped compressional wave system.

We can use the above graph in the determination of the attenuated natural frequency of the compressional wave frequency which is given to be $[\omega_n (1 - \zeta^2)^{1/2}]$.

I - (c). Attenuation Coefficient - $\gamma = \omega_n \zeta$

One of the most important aspects of the compressional wave system is that the amplitude of motion decreases exponentially with time; it is $A_0 e^{-\zeta \omega_n t}$, instead of being just A , where A_0 is the initial value of the amplitude. The amplitude decreases by a factor $\frac{1}{e}$ in a time $\frac{1}{\zeta \omega_n}$ sec., where $\zeta \omega_n = \frac{(2\mu'' + \lambda'')k^2}{2\rho}$. This length of time is a measure of how rapidly the motion is damped out by the noise and is called the modulus of decay T_n of the oscillations. The fraction of this decrease in amplitude which occurs in one cycle, i.e. the ratio between the period of vibration and the modulus of decay, is called the decrement δ of the oscillations. Another method of expressing this is in terms of the "Q of the system," where Q is the number of cycles required for the amplitude of motion to reduce to $1/e$ of its original value. If these quantities are expressed in terms of the parameters of the system, it turns out that

$$Q = \frac{1}{2\zeta} \quad \text{where } \zeta = \frac{\lambda'' + 2\mu''}{2(\lambda' + 2\mu')\rho}^{\frac{1}{2}}$$

$$T_n = \frac{1}{\omega_n \zeta} = \frac{2\rho}{(2\mu'' + \lambda'')k^2} ;$$

$$\delta = \frac{\pi}{Q} = 2\pi\zeta$$

The larger Q and T_n are, indicating that it takes a longer time for the oscillations to attenuate, and smaller δ is, indicating that the reduction in amplitude per cycle is smaller. These properties are independent of the way the system is excited.

I - (d) Quality (damping) Factor of Subbottom Soil - $Q = \frac{1}{2\zeta}$

The compressional wave system response is of the form (in frequency domain)

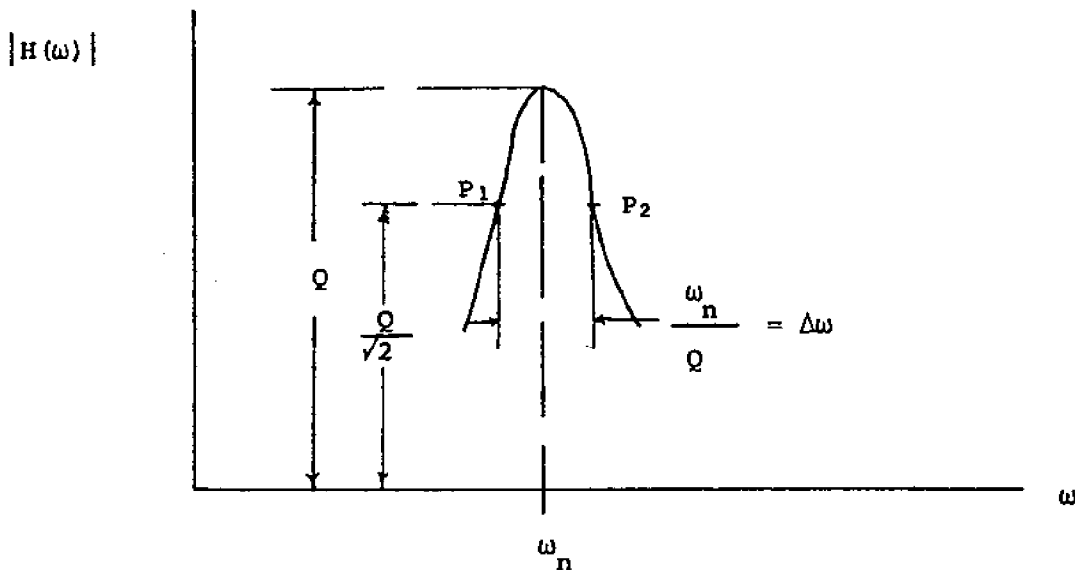
$$H(\omega) = \frac{1}{1 - \left(\frac{\omega}{\omega_n}\right)^2 + i2\zeta\frac{\omega}{\omega_n}}$$

where in terms of soil parameters

$$\omega_n = k \frac{(\lambda' + 2\mu')^{\frac{1}{2}}}{\rho^{\frac{1}{2}}} \text{ is the natural frequency of the system;}$$

$$\zeta = \frac{(\lambda'' + 2\mu'') k}{2[(\lambda' + 2\mu')\rho]^{\frac{1}{2}}} \text{ is the system attenuating constant;}$$

is sketched below.



Half Power Points and Bandwidth of a Lightly Damped
Compressional Wave System

When the damping is light i.e. the Q of the system is light, the resonance peak in $|H(\omega)|$ occurs approximately at $\omega = \omega_n$ and the curve is

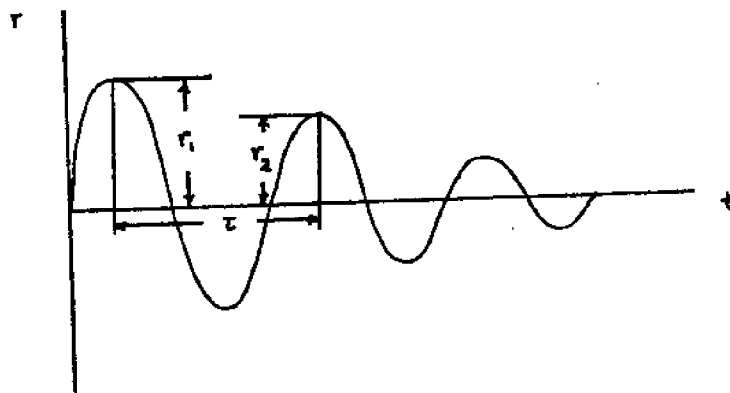
approximately $Q = \frac{1}{2\zeta}$ and the amplitude falls to 0.707 times this at the points P_1 and P_2 with frequencies $\omega_n (1 \pm 1/2Q) = \omega_n (1 \pm \zeta)$. These points are called half-power points because the power that can be absorbed by a dashpot from a simple harmonic motion at a given frequency is proportional to the square of the amplitude. The frequency difference between the half-power points is referred to as the band width of the system.

Measurement of the Damping Factor - $\zeta = \frac{k(\lambda''+2\mu'')}{2[(\lambda'+2\mu')\rho]^{1/2}}$

The compressional wave system response in time domain is of the form

$$r(t) = A_0 e^{-(\zeta\omega_n)t} \sin [(1-\zeta^2)^{1/2} \omega_n t]$$

where A_0 , $\zeta\omega_n$, and $\omega_n(1-\zeta^2)^{1/2}$ are as defined in section I-b and is represented graphically below.



Rate of decay of oscillation is measured by the logarithmic decrement.

We would like to determine the amount of damping, ζ , present in the compressional wave system by measuring the rate of decay of oscillation. This is easily achieved by a term called logarithmic decrement, which is defined as the logarithm of the ratio of any two successive amplitudes.

The logarithmic decrement δ is expressed mathematically as

$$\delta = \ln \frac{r_1}{r_2} = \ln \frac{e^{-\zeta\omega_n t_1}}{e^{-\zeta\omega_n (t_1 + \tau)}} = \ln e^{\zeta\omega_n \tau} = \zeta\omega_n \tau$$

Since the period of damped oscillation is equal to (from section I-b)

$$\tau = \frac{2\pi}{\omega_n (1-\zeta^2)^{1/2}}$$

the decrement can also be written in terms of ζ as

$$\delta = \frac{2\pi\zeta}{(1-\zeta^2)^{1/2}}$$

and in terms of soil parameters as

$$\delta = \frac{\pi (\lambda''+2\mu'')k}{[(\lambda'+2\mu')\rho]^{1/2} \left[1 - \frac{k^2(\lambda''+2\mu'')^2}{4(\lambda'+2\mu')\rho}\right]^{1/2}}$$

Similarly, the damping factor can be written in terms of δ as

$$\zeta = \frac{\delta}{(4\pi^2+\delta)}$$

and in terms of soil parameters as

$$\zeta = \frac{k(\lambda''+2\mu'')}{2[(\lambda'+2\mu')\rho]^{1/2}}$$

It should be noted that we have shown how to determine the damping factor ζ of the compressional wave system response in frequency domain by the use of Q , the quality factor of subbottom soil as indicated in section I-d and also in time domain by the use of the logarithmic decrement δ . Theoretically, these two methods should give the same damping factor for the subbottom soil. Furthermore, these two methods could be used in checking the consistency of our results.

